Polymer Journal (2014) 46, 511–515

www.nature.com/pj

NOTE

Regular assembly of filamentous viruses and gold nanoparticles by specific interactions and subsequent chemical crosslinking

Toshiki Sawada[1], Huanhuan Chen[2], Naoto Shirakawa[2], Sungmin Kang[1], Junji Watanabe[1] and Takeshi Serizawa[1]

Polymer Journal (2014) **46,** 511–515; doi:10.1038/pj.2014.38; published online 28 May 2014

Keywords: filamentous virus; gold nanoparticle; liquid crystal; self-assembly

INTRODUCTION

The molecular assembly of building blocks into regular structures has become the focus of many scientific fields. The production of regularly assembled structures in a controlled manner leads to materials with notably excellent properties with great potential in many fields, including nanotechnology and materials science. In particular, biomolecular-based assemblies exhibit better control over the assembly of structures due to their monodispersity and are utilized in diverse material fields.[1,2] Among the various biomolecules, recent studies have revealed that genetically engineered viruses offer versatile and unique properties for the construction of regularly assembled structures through self-driven processes.[3]

Recent studies have demonstrated that filamentous M13 phages act as components for use in the construction of viral materials for electronics, biodevices and sensors.[4–7] In these cases, molecular recognition capabilities are derived from the displayed foreign peptides, which specifically bind to artificial materials and have an important role in regularly assembled phage structures. Significantly, surface modification of M13 phages has been established through genetic engineering[8] and synthetic chemical[9] methods. Therefore, M13 phages are regarded as potential components of assembled nanomaterials.

In recent nanotechnological developments, regularly assembled gold nanoparticles (GNPs) have been extensively studied owing to their unique physical properties, which can be used in potential applications such as plasmonics, nanoelectronics and sensing devices.[10,11] Although there are successful approaches described in the literature for producing regularly assembled GNPs through bottom-up processes using an anisotropic lattice and the subsequent reduction of the surface energy,[12,13] such assembly requires delicate and careful control of the individual building blocks at the molecular level. Because the local ordering of GNPs affects their physical properties and applicability, strategies to control assembled structures have been developed to utilize the expressed properties relevant to assemblies.[13]

Herein, we demonstrate regular assemblies composed of M13 phages displaying gold-binding A3 peptides[14] at the phage termini (A3 phages) and the GNPs (Figure 1) based on specific interactions between A3 peptides at the phage termini and the GNP surfaces, as well as the subsequent chemical crosslinking of the phages. The GNPs formed well-organized structures in mixed solutions of A3 phages and GNPs. When crosslinking was performed between the A3-phage molecules, the mixed solutions were transformed into hydrogels. In the resultant hydrogel assemblies, A3 phages behaved as liquid crystals with domain sizes at the subcentimeter scale and the assembled GNP structures were changed. Assemblies composed of M13 phages and GNPs give rise to novel opportunities for the construction of regular assemblies as components of functional materials.

EXPERIMENTAL PROCEDURES

Preparation of gold-binding peptide-displaying phages

A3 peptides (sequence: AYSSGAPPMPPF) with gold-binding capabilities[14] were genetically fused to pIII minor coat proteins of M13 phages via Gly-Gly-Gly-Ser spacers using the Ph.D. Peptide Display Cloning System (New England Biolabs, Ipswich, MA, USA). Constructs were heat-shocked into competent *Escherichia coli* ER2738 cells. The expressed phages were purified by precipitation and redispersion procedures in the presence of high concentrations of PEG and NaCl (concentrations are 5% (w/v) and 2.5 M, respectively). Each phage displayed plural (3–5) copies of A3 peptides, and the constructs were confirmed by DNA sequencing.

Construction of assemblies composed of phages and GNPs

Citrate-capped GNPs (diameter: 15 nm, Tanaka Kikinzoku Kogyo, Tokyo, Japan) were purified twice by centrifugation and redispersion procedures using

[1]Department of Organic and Polymeric Materials, Graduate School of Science and Engineering, Tokyo Institute of Technology, Tokyo, Japan and [2]Department of Chemistry and Biotechnology, Graduate School of Engineering, The University of Tokyo, Tokyo, Japan
Correspondence: Professor T Serizawa, Department of Organic and Polymeric Materials, Graduate School of Science and Engineering, Tokyo Institute of Technology, 2-12-1-H121 Ookayama, Meguro-ku, Tokyo 152-8550 Japan.
E-mail: serizawa@polymer.titech.ac.jp
Received 28 February 2014; revised 30 March 2014; accepted 1 April 2014; published online 28 May 2014

ultrapure water. A3 phages or wild-type phages in concentrated *N*,*N*-(bis(2-hydroxyethyl)-2-aminoethane (BES) buffer were added to the GNPs solution, and the resulting solutions were incubated at 20 °C for 30 min (final conditions of the BES buffer: 50 mM BES, 150 mM NaCl and pH 7.5). The final phage and GNP concentrations were 600 and 20 nM, respectively. For chemical crosslinking of the phages, the mixed solutions were injected vertically into a 5% glutaraldehyde solution at a rate of 30 μm min^{-1} using syringes or micropipettes of various diameters and were then incubated for 2 h. Next, the resulting assemblies were transferred into BES buffer, and their stability was visually observed for 30 days.

Absorption spectrum measurements

The absorption spectra of mixed solutions composed of phages and GNPs were recorded using a NanoDrop 2000c (Thermo Scientific, Waltham, MA, USA) instrument. When chemically synthesized A3 peptides were used, concentrated A3-peptide solutions were added to the mixed solutions (final concentration: 1 mM).

Transmission electron microscopy observations

A collodion-coated copper EM grid was placed coated-side down onto mixed solutions composed of phages and GNPs or crosslinked hydrogels. Next, the grid was washed by floating on a droplet of ultrapure water for 1 min. The grids were blotted and then allowed to dry gradually at ambient temperature overnight. All images were taken using an H-7650 (Hitachi High-Tech, Tokyo, Japan) transmission electron microscope operating at 100 kV.

Polarized optical microscopy observations

Chemically crosslinked phages with and without GNPs were mounted onto glass slides. When a sample without crosslinking was observed, mixed solutions of A3 phages and GNPs were mounted onto glass slides and a cover plate with a gap of 20 μm was placed onto the samples. Samples were observed by polarized optical microscopy (POM) using a U-AN360P (Olympus, Tokyo, Japan) microscope at ambient temperature. Observations were performed by rotating the samples 45° for each image.

RESULTS AND DISCUSSION

A3 peptides were displayed on the minor coat proteins of the M13 phage termini by genetically engineering them to interact with the GNPs. A3 peptides originally screened as silver-binding peptides have the capability to bind to GNPs.[14] Mixtures of A3 phages and GNPs behaved as viscous solutions without precipitates. Absorption spectrum measurements were performed to characterize plasmonic interactions between GNPs in mixed solutions. Absorption spectra of

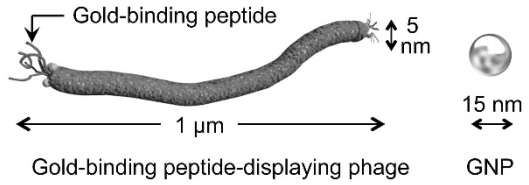

Figure 1 Schematic illustration of a filamentous M13 phage and a gold nanoparticle (GNP) used in this study. M13 phages that display gold-binding peptides at termini (A3 phages) and GNPs with a diameter of 15 nm were used. A full color version of this figure is available at *Polymer Journal* online.

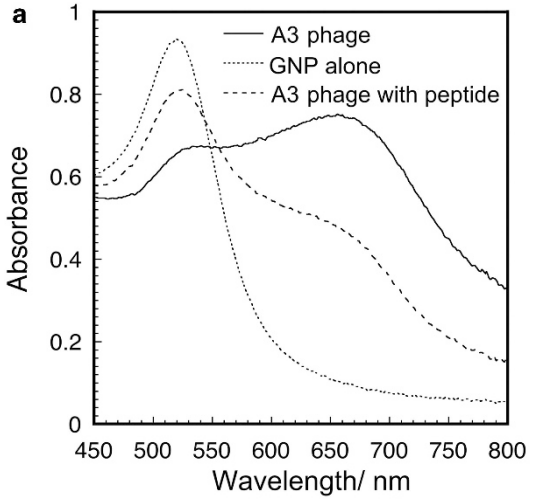

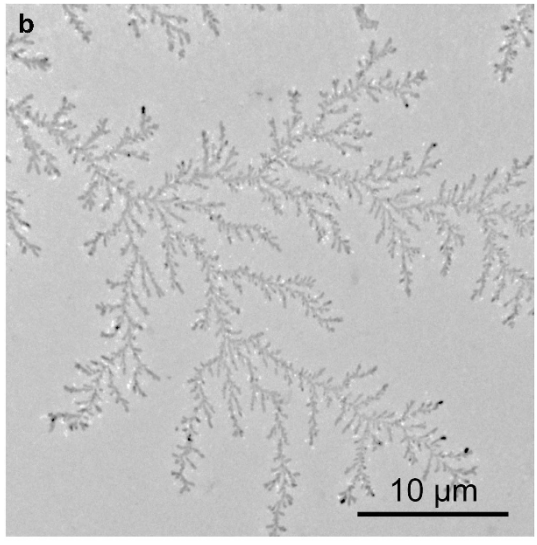

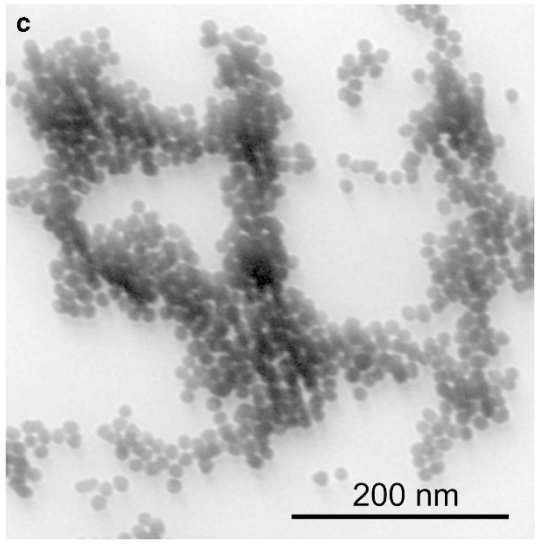

Figure 2 Characterization of regular structures of GNPs in the assemblies. (**a**) Absorption spectra of GNPs with and without A3 phages and with A3 phages combined with chemically synthesized A3 peptides. The concentrations of GNPs, A3 phages and A3 peptides were 20, 600 and 1 nM, respectively. Solid, dotted, and dashed spectra represent GNPs with A3 phages, GNPs alone and GNPs with both A3 phages and A3 peptides, respectively. (**b**) A TEM image of the regularly assembled GNPs in the mixed solutions. (**c**) A high-magnification image of the assembled GNPs. Scale bars are shown in the Figure. GNP, gold nanoparticles; TEM, transmission electron microscopy.

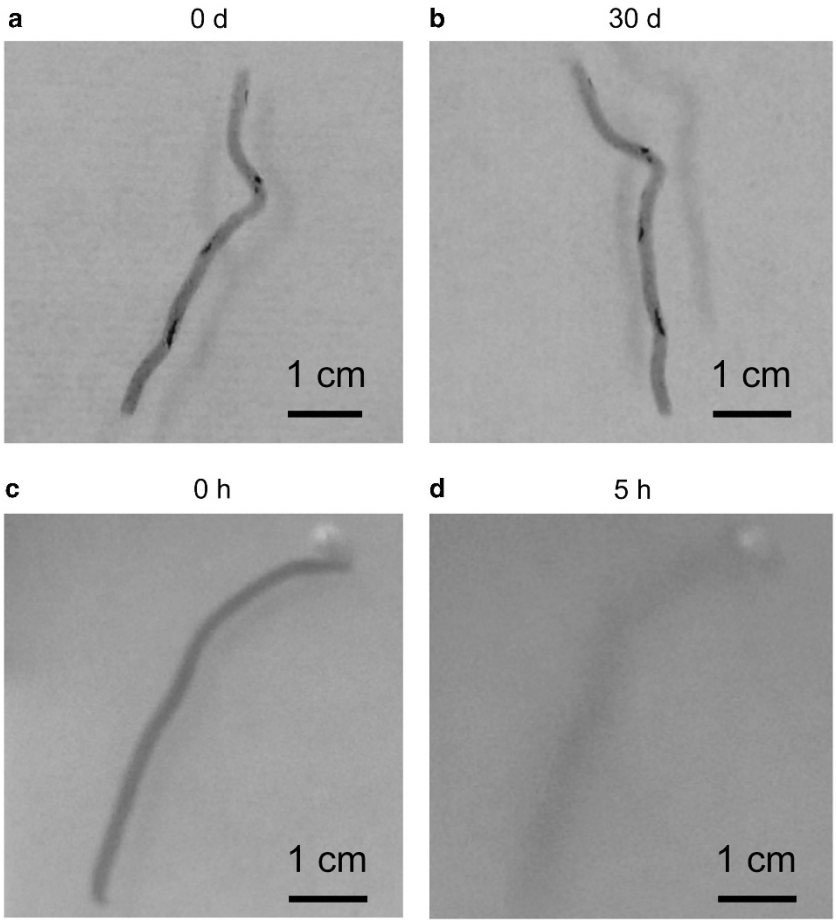

Figure 3 Photographs of gel strings. The gel strings composed of A3 phages and GNPs after chemical crosslinking incubated in buffer solutions for (**a**) 0 d and (**b**) 30 d. The strings without chemical crosslinking incubated in buffer solutions for (**c**) 0 and (**d**) 5 h. d, days. A full color version of this figure is available at *Polymer Journal* online.

GNPs with and without A3 phages are shown in Figure 2a. GNP spectra without phages exhibited a single broad band at 520 nm (Figure 2a, dotted line). Well-dispersed GNPs with a diameter of 15 nm show a λ_{max} at 520 nm.[15] Therefore, the GNPs were well dispersed in the buffered solution under these conditions. When the A3 phages interacted with GNPs, the intensity of the band at 520 nm decreased and a new broad band was observed at 600–700 nm (Figure 2a, solid line). The absorption spectra of assembled or aggregated GNPs with a diameter of 15 nm contain broad bands at 600–700 nm.[15] Furthermore, the 520-nm band indicating well-dispersed states remained, suggesting that when GNPs interact with A3 phages, they form one-dimensional-like regular structures.[16,17] Importantly, when chemically synthesized A3 peptides (final concentration: 1 mM) were added to mixed solutions composed of A3 phages and GNPs for inhibition of the interactions between the A3 peptides displayed on the A3 phages and the GNPs, the intensity of the 700-nm band decreased, while the intensity of the 520-nm band consequently increased (Figure 2a, dashed line). This observation indicated that the regular structures of GNPs formed with the A3 phages were collapsed due to the interactions of the chemically synthesized A3 peptides with the GNPs. These results suggested that interactions between the A3 peptides at the phage termini and the GNPs were fundamental to the construction of the assembly.

Transmission electron microscopy (TEM) observations were performed to directly observe the assembled GNP structures. The assembled structures were transferred to a collodion-coated grid and were subjected to TEM observations without staining. Regularly assembled structures with lengths of several tens of micrometers were observed in the TEM images for mixed solutions composed of A3 phages and GNPs (Figure 2b). The high-magnification TEM image clearly demonstrated that the regular structures were composed of GNPs (Figure 2c). When wild-type phages were used, regular structures were not observed; instead, dispersed and slightly aggregated GNPs were observed (Supplementary Figure S1). Significantly, dendritic GNP structures tended to branch out of the main chains in a similar manner. Such dendritic structures were also formed by mixing antibody-immobilized GNPs with a diameter of 20 nm and phages displaying antigen peptides at the termini.[18] Therefore, when GNPs specifically interact with the phage termini, the dendritic assembly of GNPs seems to generally occur.

Chemical crosslinking of A3 phages in mixed solutions were performed by using glutaraldehyde. When viscous solutions containing A3 phages and GNPs were spun into glutaraldehyde solutions, hydrogel strings were successfully prepared (Figure 3a). Gel strings were found to be stable in buffers for at least 30 days (Figure 3b), whereas assemblies that lacked chemical crosslinking collapsed within 5 h (Figures 3c and d). The string diameter was controlled by varying the syringe diameter (Supplementary Figure S2). Because the hydrogels were constructed by injection of the sol-state solution into a glutaraldehyde solution after formation of a viscous solution through

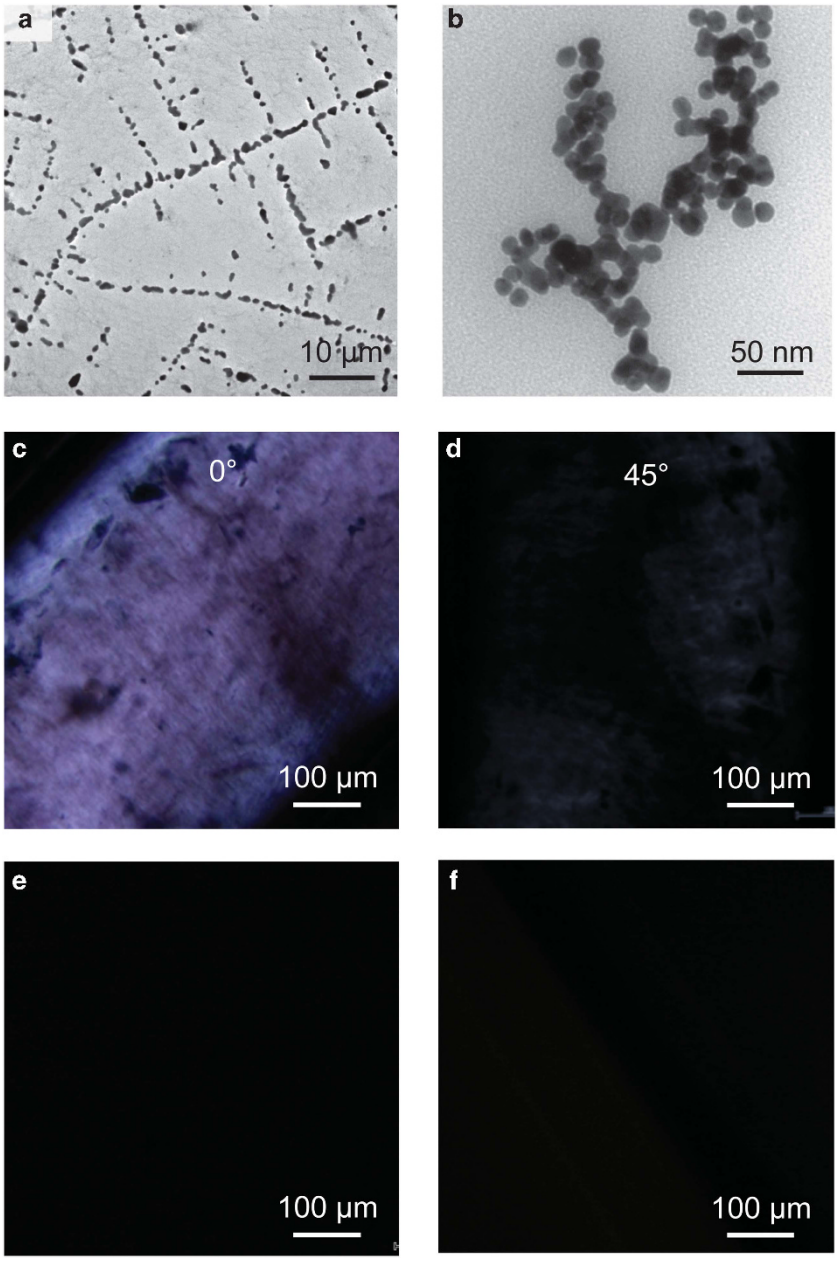

Figure 4 Characterization of crosslinked assemblies. (**a**) TEM image of regularly assembled GNPs. (**b**) A high-magnification image of the assembled GNPs. (**c**, **d**) POM images of the crosslinked assemblies composed of A3 phages and GNPs with and without 45° rotations. (**e**) POM image of the assembly without crosslinking. (**f**) POM image of crosslinked A3 phages without GNPs. GNP, gold nanoparticles; POM, polarized optical microscopy; TEM, transmission electron microscopy.

a self-assembly process, hydrogels of various shapes were generated. To investigate whether assembled structures of GNPs remained after chemical crosslinking, TEM observations were performed (Figures 4a and b). Interestingly, the perpendicularly branched assembled structures were observed to be different from those before chemical crosslinking (Figure 2b). This observation suggests that the regularity of the GNP assembly was changed by chemical crosslinking. In addition, it was difficult to avoid partially formed large aggregates of GNPs after chemical crosslinking (Figure 3a).

It is important to characterize the phage structures within the assemblies; therefore, POM observations were performed. Gel strings were mounted on glass slides, and then the gel strings were characterized using crossed-POM observations. The observation results indicated that uniform birefringence was clearly identified from the gel strings (Figure 4c). The domain size of the birefringence reached the subcentimeter scale. It is well known that the appearance of birefringence generally depends on the molecular orientation of the solute and/or the dispersion of crystalline particles;[19] therefore, highly ordered structures should be present in assembled hydrogels. The bright POM image was darkened by a 45° rotation of the samples (Figure 4d), demonstrating a lyotropic liquid crystalline formation. Given the component structure of hydrogels, filamentous A3 phages are considered to be oriented to form liquid crystals. It has been demonstrated that highly concentrated M13 phages align into

orientationally ordered structures, resulting in lyotropic liquid crystal suspensions.[20] The concentration of phages required to form liquid crystals without other additives was approximately three times greater than in the present results. Thus, specific interactions between the peptides on the phage termini and the GNPs are essential factors to form regular phage assemblies. Because birefringence was not observed in the POM images of the samples before chemical crosslinking (Figure 4e), chemical crosslinking was required to induce liquid crystal formation. Furthermore, when only A3 phages were chemically crosslinked under the same conditions, no birefringence was observed (Figure 4f). On the basis of all the POM observations, assembly by specific interactions as well as chemical crosslinking was required for the liquid crystal formation. Therefore, our results demonstrated that filamentous M13 phages and GNPs were cooperatively assembled into regular structures through specific interactions and subsequent chemical crosslinking.

CONCLUSIONS

We demonstrated the regular assembly of gold-binding peptide-displaying filamentous phages and GNPs through specific interactions and subsequent chemical crosslinking. TEM observations clearly demonstrated that the GNPs that interacted with the A3 phages in mixed solutions were self-assembled into highly regular structures. Stable assemblies composed of A3 phages and GNPs were successfully constructed by chemical crosslinking using amine coupling strategies between phages, resulting in the formation of hydrogels. The regularity of the assembled GNPs in hydrogels was altered by chemical crosslinking. Furthermore, the A3 phages in hydrogels exhibited liquid-crystalline properties, indicating that the A3 phages were highly oriented in the hydrogels. Because a number of material-binding peptides were biotechnologically obtained, various metal nanoparticles could be applied to this strategy for the construction of regular assembles. Furthermore, functional molecules could be conjugated to the surface of M13 phages by genetic engineering and synthetic methods; therefore, various functionalized assemblies could be constructed. Accordingly, our results will contribute to novel imaginative opportunities for the exploitation of structurally regular assemblies in materials science and technology.

ACKNOWLEDGEMENTS

This work was supported in part by a Grant-in-Aid for Young Scientists (B) from the Japan Society for the Promotion of Science (JSPS) (no. 11019204), a Grant for Basic Science Research Project from the Sumitomo Foundation (no. 110427), the Asahi Glass Foundation, the Japan Prize Foundation and the Mizuho Foundation for the Promotion of Science. TEM observations were supported by the Center for Advanced Materials Analysis, Tokyo Institute of Technology.

1 Ariga, K., Ji, Q., Mori, T., Naito, M., Yamauchi, Y., Abe, H. & Hill, J. Enzyme nanoarchitectonics: organization and device application. *Chem. Soc. Rev.* **42,** 6322–6345 (2013).
2 Zhang, S. Fabrication of novel biomaterials through molecular self-assembly. *Nat. Biotechnol.* **21,** 1171–1178 (2003).
3 Yang, S., Chung, W.-J., McFarland, S. & Lee, S.-W. Assembly of bacteriophage into functional materials. *Chem. Rec.* **13,** 43–59 (2013).
4 Nam, K., Kim, D.-W., Yoo, P., Chiang, C.-Y., Meethong, N., Hammond, P., Chiang, Y.-M. & Belcher, A. M. Virus-enabled synthesis and assembly of nanowires for lithium ion battery electrodes. *Science* **312,** 885–888 (2006).
5 Merzlyak, A., Indrakanti, S. & Lee, S.-W. Genetically engineered nanofiber-like viruses for tissue regenerating materials. *Nano Lett.* **9,** 846–852 (2009).
6 Souza, G., Molina, J., Raphael, R., Ozawa, M., Stark, D., Levin, C., Bronk, L., Ananta, J., Mandelin, J., Georgescu, M.-M., Bankson, J., Gelovani, J., Killian, T., Arap, W. & Pasqualini, R. Three-dimensional tissue culture based on magnetic cell levitation. *Nat. Nanotechnol.* **5,** 291–297 (2010).
7 Oh, J.-W., Chung, W.-J., Heo, K., Jin, H.-E., Lee, B., Wang, E., Zueger, C., Wong, W., Meyer, J., Kim, C., Lee, S.-Y., Kim, W.-G., Zemla, M., Auer, M., Hexemer, A. & Lee, S.-W. Biomimetic virus-based colourimetric sensors. *Nat. Commun.* **5,** 3043 (2014).
8 Smith, G. P. & Petrenko, V. A. Phage display. *Chem. Rev.* **97,** 391–410 (1997).
9 Kritzer, J., Hamamichi, S., McCaffery, J., Santagata, S., Naumann, T., Caldwell, K., Caldwell, G. & Lindquist, S. Rapid selection of cyclic peptides that reduce alpha-synuclein toxicity in yeast and animal models. *Nat. Chem. Biol.* **5,** 655–763 (2009).
10 Wilson, R. The use of gold nanoparticles in diagnostics and detection. *Chem. Soc. Rev.* **37,** 2028–2045 (2008).
11 Alkilany, A., Lohse, S. & Murphy, C. The gold standard: Gold nanoparticle libraries to understand the nano-bio interface. *Acc. Chem. Res.* **46,** 650–661 (2012).
12 Chen, C.-L. & Rosi, N. L. Preparation of unique 1-d nanoparticle superstructures and tailoring their structural features. *J. Am. Chem. Soc.* **132,** 6902–6903 (2010).
13 Shaw, C. P., Fernig, D. G. & Levy, R. Gold nanoparticles as advanced building blocks for nanoscale self-assembled systems. *J. Mater. Chem.* **21,** 12181–12187 (2011).
14 Slocik, J., Stone, M. & Naik, R. Synthesis of gold nanoparticles using multifunctional peptides. *Small* **1,** 1048–1052 (2005).
15 Liu, X., Atwater, M., Wang, J. & Huo, Q. Extinction coefficient of gold nanoparticles with different sizes and different capping ligands. *Colloids Surf. B. Biointerfaces* **58,** 3–7 (2007).
16 Sardar, R. & Shumaker-Parry, J. S. Asymmetrically functionalized gold nanoparticles organized in one-dimensional chains. *Nano Lett.* **8,** 731–736 (2008).
17 Lin, S., Li, M., Dujardin, E., Girard, C. & Mann, S. One-dimensional plasmon coupling by facile self-assembly of gold nanoparticles into branched chain networks. *Adv. Mater.* **17,** 2553–2559 (2005).
18 Sawada, T., Kang, S., Watanabe, J., Mihara, H. & Serizawa, T. Hybrid hydrogels composed of regularly assembled filamentous viruses and gold nanoparticles. *ACS Macro. Lett.* **3,** 341–345 (2014).
19 Okajima, M., Kaneko, D., Mitsumata, T., Kaneko, T. & Watanabe, J. Cyanobacteria that produce megamolecules with efficient self-orientations. *Macromolecules* **42,** 3057–3062 (2009).
20 Dogic, Z. & Fraden, S. Ordered phases of filamentous viruses. *Curr. Opin. Colloid Interface Sci.* **11,** 47–55 (2006).

Supplementary Information accompanies the paper on Polymer Journal website (http://www.nature.com/pj)